Concerted regulation of skeletal muscle contractility by oxygen tension and endogenous nitric oxide

Jerry P. Eu*, Joshua M. Hare†‡, Douglas T. Hess*‡, Michel Skaf†‡, Junhui Sun§, Isabella Cardenas-Navina¶, Qi-An Sun*, Mark Dewhirst¶, Gerhard Meissner§, and Jonathan S. Stamler*‖**

Departments of *Medicine and ¶Radiation Oncology, and ‖Howard Hughes Medical Institute, Duke University Medical Center, Durham, NC 27710; †Cardiology Division, The Johns Hopkins Hospital, Baltimore, MD 21287; and §Department of Biochemistry and Biophysics, University of North Carolina, Chapel Hill, NC 27559

Edited by Louis J. Ignarro, University of California School of Medicine, Los Angeles, CA, and approved October 2, 2003 (received for review June 6, 2003)

It is generally accepted that inhibition of nitric oxide synthase (NOS) facilitates, and thus nitric oxide (NO) inhibits, contractility of skeletal muscle. However, standard assessments of contractility are carried out at a nonphysiological oxygen tension [partial pressure of oxygen (pO_2)] that can interfere with NO signaling (95% O_2). We therefore examined, in normal and neuronal NOS (nNOS)-deficient mice, the influence of pO_2 on whole-muscle contractility and on myocyte calcium flux and sarcomere shortening. Here, we demonstrate a significant enhancement of these measures of muscle performance at low physiological pO_2 and an inhibitory influence at higher physiological pO_2, which depend on endogenous nNOS. At 95% O_2 (which produces oxidative stress; muscle core pO_2 ≈400 mmHg), force production is enhanced but control of contractility by NO/nitrosylation is greatly attenuated. In addition, responsivity to pO_2 is altered significantly in nNOS mutant muscle. These results reveal a fundamental role for the concerted action of NO and O_2 in physiological regulation of skeletal muscle contractility, and suggest novel molecular aspects of myopathic disease. They suggest further that the role of NO in some cellular systems may require reexamination.

It has recently been recognized that redox-based regulation of protein function serves not only to mediate compensatory responses to oxidative or nitrosative stress but also modulates transduction along basic signaling pathways in mammalian cells (1). Further, accumulating evidence indicates that nitric oxide (NO)-based protein modifications are critical effectors of redox regulation, which may be linked at the molecular level to partial pressure of oxygen (pO_2) (1). Accordingly, the functional contribution of redox mechanisms remains, for the most part, untested, and potentially masked in virtually all *ex vivo* studies, which have been carried out at supranormal oxygen tension (typically 21% O_2 for cells and 95% O_2 for tissue, whereas pO_2 *in vivo* is much lower).

Mammalian skeletal muscle operates over a range of pO_2, which is determined by local blood flow and muscle activity, and contains endogenous sources of NO. The μ-isoform of type I or neuronal NO synthase (nNOS) localizes to the plasma membrane (sarcolemma) of skeletal muscle fibers through interaction with the dystrophin complex (2–4). In many mammals, nNOS is either restricted to or particularly abundant in fast-twitch fibers, although, in humans, fast- and slow-twitch fibers are more evenly endowed (2, 5, 6). The loss of nNOS from sarcolemma of *mdx* mice (whose fast-twitch fibers are disproportionately impaired), and of patients with Duchenne or Becker muscular dystrophy, focused interest on the possibility that NO produced by muscle fibers may play a role in excitation–contraction (E–C) coupling and that NO deficiency may contribute to contractile impairment in muscle disease (2–6). However, although mice deficient in nNOS show subtle abnormalities in muscle blood flow (7), overt alterations in contractile function have not been described.

Studies of isolated skeletal muscle have generally been carried out at grossly nonphysiological oxygen tension, usually 95% O_2, whereas skeletal muscle pO_2 is in the range from 4 to 20 mmHg (0.5–2.5% O_2), and even lower in working muscle (8, 9). Supranormal O_2 concentrations have been shown *in vitro* to disrupt regulation by NO of the ryanodine receptor/calcium release channel (RyR1) of skeletal muscle sarcoplasmic reticulum (SR) (10). Therefore, to reveal the physiological role of O_2/NO in regulation of muscle function, we examined, over a range of pO_2, the contractile properties and calcium flux/sarcomere shortening, respectively, of isolated predominantly fast-twitch whole-muscle [extensor digitorum longus (EDL)] and single myocytes [flexor digitorum brevis (FDB)] obtained from normal and from genetic knockout mice in which nNOS is selectively absent ($nNOS^{-/-}$) (11).

Experimental Procedures

Muscle Bioassay. EDL muscles were obtained from male mice at 6–8 weeks of age ($nNOS^{-/-}$ and C57BL/6, The Jackson Laboratory). Each experiment used the left and right EDL from a single mouse, which were removed and suspended from proximal and distal tendons, in series with force transducers, in organ baths at 37°C containing Krebs' solution supplemented with D-tubocurarine (25 μM; to eliminate any influence of neuromuscular transmission). Muscles were allowed to equilibrate for ≈15 min at 5% CO_2 and either 1–2% O_2, 20% O_2, or 95% O_2. Bath oxygen tension was monitored with an oxygen electrode (WPI Instruments, Waltham, MA). When used, L-nitroarginine methyl ester (L-NAME) (1 mM) was added to the bath at the beginning of the equilibration period. All measurements of muscle pairs were carried out in parallel. Contractions were elicited by square-wave constant-voltage stimulation (50–80 V) of 2 msec duration through 7.0-mm-wide platinum electrodes placed parallel to the long axis of the muscle. Before testing, each muscle was adjusted to the length at which isometric twitch-force generation was maximal (optimum muscle length, L_o). At least 2 min elapsed between single-twitch stimuli, and between trains of tetanic stimuli, and tetanic testing always followed the completion of single-twitch measurements. Tetanic stimulation consisted of pulse trains of 75 msec duration, and the amplitude of individual stimuli was set at a level equal to either half-maximal or maximal single-twitch stimulation. For each muscle, L_o was measured after the final tetanic stimulation, the muscle was weighed wet, and the effective cross-sectional area was calculated by approximating the muscle as a cylinder of length, L_o, and a density of 1.06 gm/cm^{-3} (12). Because L_o did not differ significantly between WT and $nNOS^{-/-}$ EDL (1.35 ± 0.06 cm vs.

This paper was submitted directly (Track II) to the PNAS office.

Abbreviations: NOS, NO synthase; nNOS, neuronal NOS; pO_2, partial pressure of oxygen; E–C, excitation–contraction; SR, sarcoplasmic reticulum; RyR1, ryanodine receptor/calcium release channel; EDL, extensor digitorum longus; FDB, flexor digitorum brevis; L-NAME, L-nitroarginine methyl ester.

‡J.M.H., D.T.H., and M.S. contributed equally to this work.

**To whom correspondence should be addressed at: Department of Medicine, Box 2612, Duke University Medical Center, Durham, NC 27710. E-mail: staml001@mc.duke.edu.

Table 1. EDL muscle core pO_2 in tissue baths sparged with O_2

O_2, %	Muscle pO_2, mmHg
1	3.5 ± 2.4
20	40.7 ± 6.5
95	387 ± 19.1

Measured with an oxygen electrode. Results are mean ± SE; $n = 4$.

1.36 ± 0.06 cm, $P = 0.77$), differences in effective cross-sectional area were largely a result of differences in muscle mass. Between-group analyses of single or multiple parameters were carried out, respectively, with Student's t test and ANOVA.

Measurement of Muscle pO_2. EDL muscles were fixed horizontally in Krebs' solution bubbled continuously with 20% O_2/5% CO_2. A polaragraphic oxygen electrode (glass micropipette; tip diameter ≈10 μm), calibrated after each use, was used to measure pO_2 after penetration of the muscle core (13). The composition of the sparging gas was changed sequentially from 20% O_2 to 95% O_2 and 1% O_2 after equilibration at each pO_2 (≈10 min).

Myocyte Ca^{2+} Transients and Sarcomere Shortening. FDB muscles obtained from C57BL/6 and *nNOS*$^{-/-}$ mice were incubated with 2% collagenase type 2 (Worthington Lab) for 18 h at 37°C under 95%O_2/5% CO_2 before myocytes were dispersed and stored until use in Tyrodes solution containing 1.8 mM Ca^{2+} at room temperature. For experimental observations, myocytes were transferred to a sealed microscope stage compartment and superfused continuously at room temperature with Tyrodes solution containing 1.8 mM Ca^{2+} and 0.5 mM probenecid. Observations were obtained first at 20% O_2 before adjustment to 1% O_2. Depolarizing stimulation (pacing) was delivered continuously at 0.5 Hz. Measurement of intracellular Ca^{2+} and of sarcomere length were as described (14). Ca^{2+} measurement used Fura-2/AM (5 μM) and a dual-wavelength spectrophotometer exciting alternately at 365 and 380 nm. Sarcomere length was monitored continuously with a charge-coupled device camera and changes in sarcomere length were determined by fast Fourier transform of the Z-line density trace.

Results

We first compared the contractile properties of EDL at a physiologically extreme bath oxygen tension of 20–21% O_2 (pO_2 ≈150 mmHg, ambient pO_2), which represents an oxidative stress for peripheral tissue, and at 1–2% O_2 (pO_2 ≈10 mmHg), which is characteristic of normal mammalian striated muscle *in vivo* (8, 9). Direct measurement at the muscle core (see *Experimental Procedures* and Table 1) indicated that mean muscle pO_2 was ≈40 mmHg (median 36.7 mmHg) at 20% bath O_2 and ≈3.5 mmHg (median 1.75 mmHg) at ≈1–2% bath O_2. Thus, 1–20% bath O_2 recapitulates the physiological O_2 gradient in skeletal muscle (8, 9). In addition, to allow a direct comparison with previous results, we examined EDL performance at 95% bath O_2 (pO_2 ≈700 mmHg), in which we measured a core pO_2 ≈400 mmHg, thus eliminating the physiological O_2 gradient (Table 1). Some measurements of muscle performance were obtained sequentially at different oxygen tensions to examine the time course and reversibility of pO_2-dependent changes in contractility (see Fig. 2*A*).

We assessed fundamental measures of E–C coupling and force production, isometric and tetanic twitch tensions, for muscles adjusted along their length-tension curve to optimize force generation. Measurements of force evoked by single-pulse stimulation revealed that, with stimuli producing about half-maximal twitch tension, the force generated by EDL was increased by ≈45% at 1% vs. 20% O_2, and even for stimuli producing maximal

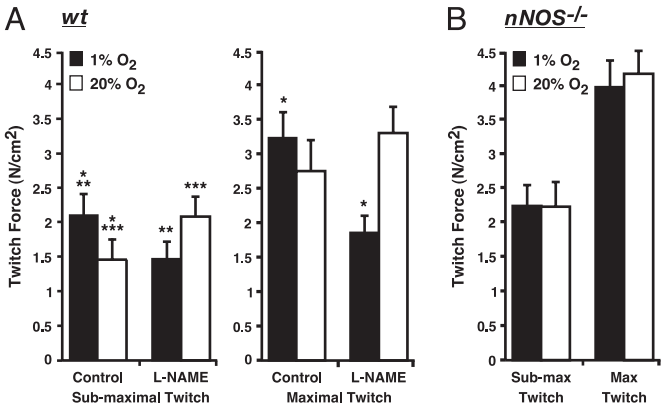

Fig. 1. Isometric twitch tension evoked by maximal or approximately half-maximal single-twitch stimulation of EDL from WT (*A*) or *nNOS*$^{-/-}$ (*B*) mice, at 1% or 20% O_2, and in the presence or absence of the NOS inhibitor, L-NAME. Histograms illustrate force production normalized for EDL cross-sectional area (M/cm^2). Each bar represents measurements obtained from 8–10 individual EDL muscles. (*A*) For submaximal stimulation, significance was attained ($P < 0.05$) by the increase in twitch force at 1% vs. 20% O_2 in the absence of L-NAME (*), by the decrease in twitch force at 1% O_2 in the presence vs. absence of L-NAME (**) and by the increase in twitch force at 20% O_2 in the presence vs. absence of L-NAME (***). At maximal twitch tension, the L-NAME-induced decrease in twitch force at 1% O_2 was significant. (*B*) Twitch force was independent of pO_2 in EDL from *nNOS*$^{-/-}$ mice. Note that maximal twitch force was significantly greater in nNOS$^{-/-}$ EDL (*B*) vs. WT EDL (*A*) at both 1% and 20% O_2 and that this increase was also significant for submaximal twitch force at 20% O_2 ($P < 0.05$).

twitch tensions, twitch tension amplitude was ≈20% greater at low pO_2 ($P < 0.05$; Fig. 1*A*). These observations reveal pO_2-dependent regulation of E–C coupling, and recent findings provide a likely mechanism: NO modifies by S-nitrosylation a single cysteine residue (Cys-3635) within RyR1 and thereby augments substantially Ca^{2+} flux through RyR1, which governs active contraction (10, 15). Remarkably, NO acts on this critical thiol only at physiological O_2 concentrations (≈10 mmHg or less), where the pO_2-dependent redox state of a small subset of RyR1 thiols (representing an O_2 sensor) is reduced, thereby producing an NO-responsive conformation in the channel (10). In contrast, NO has no effect at supranormal pO_2, where these allosteric effector thiols are oxidized. Thus, mechanistic analysis of NO effects on RyR1 indicates that NO should facilitate contractility at low physiological pO_2. In contrast, the original analysis of diaphragm muscle (5, 16) and subsequent studies (reviewed in ref. 6), all carried out at supraphysiological pO_2, have reported consistently that pharmacologic inhibition of NOS enhances force production by skeletal muscle *ex vivo* (i.e., NO is inhibitory).

We reassessed directly the role of endogenous NO in pO_2-dependent regulation of contractility employing both *nNOS*$^{-/-}$ mice and acute inhibition of NOS with L-NAME. The isometric twitch tensions developed by EDL from *nNOS*$^{-/-}$ mice were indistinguishable at 1% or 20% O_2, with either submaximal or maximal stimulation (Figs. 1*B* and 2*B*). Thus, in the absence of endogenous NO production by nNOS, the influence of pO_2 on twitch tension is completely eliminated. This finding, in combination with the increase in twitch tension at low vs. high pO_2 in WT EDL (Fig. 1*A*), indicates a concerted influence of pO_2 and NO that results in the enhancement by endogenous NO of E–C coupling and force production at physiological oxygen tension. In addition, we observed that *nNOS*$^{-/-}$ EDL generated greater twitch force than did WT EDL (normalized for cross-sectional area), at both low and high pO_2 (Fig. 1). At 1% O_2, this increase was nonsignificant for half-maximal twitch tension, but maximal

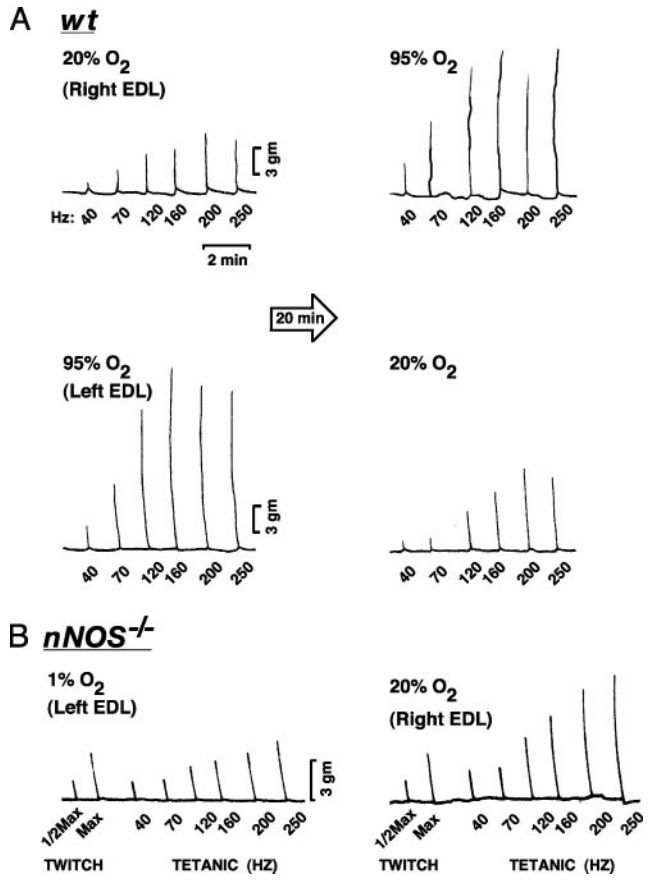

Fig. 2. Reversibility and NO/O_2 regulation of twitch and tetanic force production by the left and right EDLs from an individual WT and an individual *nNOS*$^{-/-}$ mouse. (*A*) Strain gauge recordings from a pair of simultaneously assayed WT EDLs illustrate the rapid and bidirectional changes in tetanic twitch tension after switching between 20% and 95% O_2 [maximum force at 95% O_2 (left EDL) = 36 M/cm^2]. (*B*) Records from a pair of simultaneously assayed *nNOS*$^{-/-}$ EDLs illustrate that neither half-maximal nor maximal twitch tension differs at 1% vs. 20% O_2, whereas tetanic force generation is substantially greater at 20% O_2 than at 1% O_2 (see also Figs. 1*B* and 3*D*).

twitch force was increased by ≈22%, and at 20% O_2, twitch force increased by ≈54% for both submaximal and maximal twitch tensions ($P < 0.05$). These observations indicate the operation of distinct NO-independent compensatory force-enhancing mechanisms that are regulated by O_2 in fast-twitch muscle deprived chronically of nNOS activity.

The effects on twitch tension of acute NOS inhibition provided additional evidence for concerted regulation by NO and O_2 of EDL function (Fig. 1*A*). At a physiological O_2 concentration of 1% O_2 (characteristic of active muscle), L-NAME treatment (1 mM) reduced half-maximal and maximal twitch force by 30% and 42%, respectively ($P < 0.05$), which is closely comparable to the difference between twitch tensions obtained at 1% and 20% O_2. Thus, consistent with the results from EDL of *nNOS*$^{-/-}$ mice, the magnitude of the NO-dependent enhancement of contractility revealed by L-NAME accounts fully for the potentiating effects on twitch tension of low vs. high pO_2. In striking contrast, but consistent with previous observations (5, 6, 16), twitch force was enhanced by L-NAME at 20% O_2, resulting in increases of 43% and 24% for submaximal and maximal twitch tensions, respectively ($P < 0.05$; Fig. 1*A*). The enhancement of force production by NOS inhibition in the ambient air condition (≈40 mmHg) indicates that at higher physiological pO_2 (associated with relative muscle inactivity), NO exerts an inhibitory influence on the contractile apparatus. The mechanism of action is unlikely to involve a direct modulation of Ca^{2+} release from the SR because RyR1 is not modified by NO at supranormal pO_2 (10, 15).

We also examined the response of EDL to trains of stimuli that produce tetanic (fused) contractions, and, which, relative to single-twitch stimulation, will evoke large and sustained increases in cytosolic Ca^{2+} levels and NO production (6). We used pulse trains comprised of individual pulses with amplitudes corresponding to either half-maximal or maximal single-twitch stimulation, and in no case did stimulus amplitude influence the reported effects of pO_2 or of NO. In addition, it should be noted that, although maximal tetanic tension developed at stimulus rates of 200–250 per sec under all conditions (Figs. 2 and 3), observations in intact, behaving rodents indicate that the physiological range of sustained discharge of motor neurons supplying fast-twitch muscles of the limb extends only through ≈100 per sec (17, 18), which in fact encompasses the range over which we observed the largest NO/O_2-dependent differences in contractility (*vide infra*).

Normalized force frequency curves obtained from WT EDL at 1% vs. 20% O_2 did not differ significantly over the measured tetanic frequency range of 40–250 Hz. (Fig. 3A). However, consistent with the pO_2-dependent effects of acute NOS inhibition on twitch tension (Fig. 1*A*), treatment with L-NAME resulted in a leftward shift of the force frequency relationship at 20% O_2 and a rightward shift at 1% O_2 (Fig. 3*A*). The difference between the normalized force frequency curves at 1% O_2 and 20% O_2 after L-NAME treatment was significant over the physiologically relevant range of 40–120 Hz ($P < 0.05$). More strikingly, plots of absolute force vs. stimulation frequency revealed that acute NOS inhibition produced substantial increases in tetanic force at 20% O_2 (Fig. 3*B*), which averaged 68% and were significant over the frequency range of 40–120 Hz vs. both 20% O_2 in the absence of L-NAME ($P < 0.05$; Fig. 3*B*) and 1% O_2 in the presence or absence of L-NAME ($P < 0.05$; Fig. 3*B*). Force generation/stimulation frequency curves obtained at 20% O_2 in the absence of L-NAME were not significantly different from 1% O_2 in the presence of L-NAME and 1% O_2 in the absence of L-NAME (Fig. 3*B*). Tetanic force generation by WT EDL at 95% O_2 was substantially greater than at 1% O_2 or 20% O_2 (with peak tensions of ≈35–40 M/cm^2, which is equivalent to ≈20 g; Figs. 2*A* and 3 *B* and *C*), but, whereas L-NAME treatment yielded a small but significant leftward shift in the normalized force frequency curves at lower stimulus frequencies (consistent with previous findings at 95% O_2; refs. 5, 6, and 12), no significant differences were obtained between absolute force vs. frequency curves at 95% O_2 in the presence vs. absence of L-NAME (Fig. 3 *C* and *D*). Thus, the inhibitory influence of NO on force production evident at 20% O_2 (≈40 mmHg) is no longer exerted in the extreme redox environment created <95% O_2 (≈400 mmHg). Taken together, the effects of NOS inhibition on contractile responses to repetitive stimulation indicate that the influence of NO varies with pO_2 and muscle activation, which will conjointly determine the redox milieu of critical subcellular compartments (19, 20).

Normalized force-frequency curves from EDL of *nNOS*$^{-/-}$ mice were essentially indistinguishable at 1%, 20%, and 95% O_2 (Fig. 3 *E* and *H*). Thus, in the chronic absence of nNOS-derived NO, pO_2 exerts no influence on the form of the force-frequency relationship obtained by repetitive stimulation. In addition, L-NAME had no significant effect on either normalized or absolute force frequency curves from *nNOS*$^{-/-}$ mice (Fig. 3 *G* and *H*). However, consistent with the increase in twitch force generated by EDL of *nNOS*$^{-/-}$ vs. WT (Fig. 1*B*), tetanic force production by EDL of *nNOS*$^{-/-}$ mice at 20% O_2 (Figs. 2*B* and 3*F*) was greater than at 1% O_2 and exceeded force generation by WT EDL at 1% or 20% O_2 ($P < 0.05$; tetanic force production

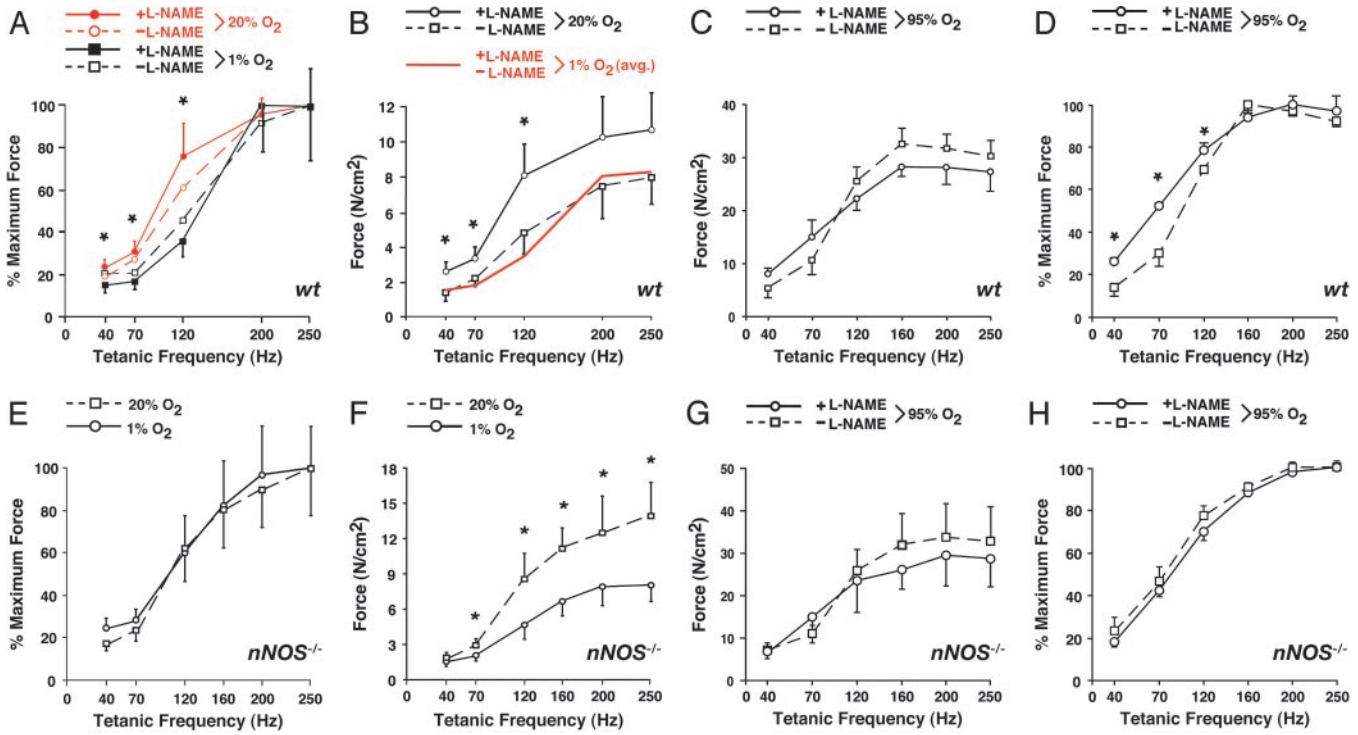

Fig. 3. Contractile force evoked by tetanic stimulation (40–250 Hz) of EDL from WT (*A–D*) and *nNOS*$^{-/-}$ (*E–H*) mice at 1%, 20%, or 95% O_2, and in the presence or absence of the NOS inhibitor, L-NAME. All significant differences ($P < 0.05$) are indicated by asterisks. (*A*) Normalized force frequency curves illustrate that, in WT mice, L-NAME induces a leftward (facilitatory) shift at 20% O_2 and a rightward (inhibitory) shift at 1% O_2. Significant differences were obtained between the curves at 1% and 20% O_2 in the presence of L-NAME over the stimulation range of 40–120 Hz (SE indicated only for measurements in the presence of L-NAME). (*B*) Plots of force generation vs. stimulation frequency illustrate that force production is enhanced significantly at 20% O_2 in the presence vs. absence of L-NAME over the stimulation range of 40–120 Hz. There were no significant differences between force generation/stimulation-frequency curves obtained at 20% O_2 in the absence of L-NAME, 1% O_2 in the absence of L-NAME, and 1% O_2 in the presence of L-NAME, and, for clarity, the averaged curve for 1% O_2 in the absence and presence of L-NAME is shown in red. (*C*) At 95% O_2, L-NAME treatment has no significant effect on force generated by tetanic pulse trains but results in a leftward (facilitatory) shift in normalized frequency force curves at 70–120 Hz (*D*). (*E–H*) EDL from *nNOS*$^{-/-}$ mice. Normalized force frequency curves are essentially indistinguishable at 1% vs. 20% O_2 (*E*), but force generation is enhanced significantly at 20% vs. 1% O_2 over the stimulation range of 70–250 Hz (*F*). L-NAME has no significant effect on *nNOS*$^{-/-}$ EDL contractility, as illustrated with results obtained at 95% O_2 (*G* and *H*). Note that, as for WT EDL, force generation by *nNOS*$^{-/-}$ EDL is greater at 95% O_2 than at 20% or 1% O_2, but that force production by WT EDL and *nNOS*$^{-/-}$ EDL is comparable at 95% O_2.

did not differ significantly between *nNOS*$^{-/-}$ EDL at 1% O_2, WT EDL at 1% O_2, and WT EDL at 20% O_2). Thus, pO_2-dependent differences in force generation were revealed in the absence of nNOS as well as by acute NOS inhibition (Fig. 3 *A* and *B*). Furthermore, the pO_2-dependent difference in force generation by EDL from *nNOS*$^{-/-}$ mice increased with increasing tetanic stimulus frequency (Figs. 2*B* and 3*F*). As for WT EDL, force generation by *nNOS*$^{-/-}$ EDL was greater at 95% O_2 than at 1% O_2 and at 20% O_2 (Fig. 3 *F* and *G*). It should be noted that at 95% O_2, force production by *nNOS*$^{-/-}$ EDL and WT EDL was similar (Fig. 3 *C* and *G*), i.e., the enhanced contractility of *nNOS*$^{-/-}$ EDL at low and intermediate pO_2 is much less evident at grossly supranormal oxygen tension. These observations establish that tetanic force generation is increased in *nNOS*$^{-/-}$ muscle at higher physiological pO_2 and suggest that mechanisms operating to increase force production may include increased generation of or sensitivity to force-enhancing factors, such as reactive oxygen species (ROS, which may be produced in greater quantities with increasing pO_2 and muscle activation), and that pathological amounts of ROS may obscure redox signaling (19, 20). We have observed only minimal effects of Cu/Zn superoxide dismutase, applied to intact muscle (19), on force production by EDL (unpublished results), but a role for ROS generated and acting intracellularly remains to be examined.

A direct demonstration of concerted regulation by pO_2 and NO of both Ca^{2+} flux and contractile function was provided by analysis of depolarization-induced changes in cytoplasmic Ca^{2+} levels and sarcomere length in myocytes isolated from FDB (of WT and *nNOS*$^{-/-}$ mice and examined at 1% O_2 and 20% O_2 (14) (Fig. 4). Both calcium transients and sarcomere shortening evoked by brief electrical stimulation were significantly greater at 1% O_2 than at 20% O_2 in myocytes derived from WT FDB ($P < 0.05$), whereas pO_2 had no effect on either measure in *nNOS*$^{-/-}$ myocytes. In addition, both the amplitude of Ca^{2+} transients and the magnitude of sarcomere shortening were significantly greater at 20% O_2, but not at 1% O_2, in *nNOS*$^{-/-}$ vs. WT myocytes ($P < 0.05$). Thus, these observations confirm at the level of single muscle cells both the facilitatory action of NO on contractility at low physiological pO_2 and the pO_2-regulated compensatory enhancement of contractile function in *nNOS*$^{-/-}$ muscle. At the molecular level, the pO_2-dependent influence of NO on Ca^{2+} transients, which are known to reflect primarily Ca^{2+} release through RyR1 (21), supports a role for RyR1 as a principal locus of action in concerted redox regulation by pO_2 and NO (10, 15).

Discussion

Our findings demonstrate that skeletal muscle contractility varies with oxygen tension and that this pO_2-dependent modulation is effected in substantial part through the action of NO generated by nNOS *in situ*. Concerted regulation by NO and O_2 of E–C coupling and force production operates at both low- and high-oxygen tension. The influence of NO at low physiological pO_2 is facilitatory, whereas NO inhibits contractility

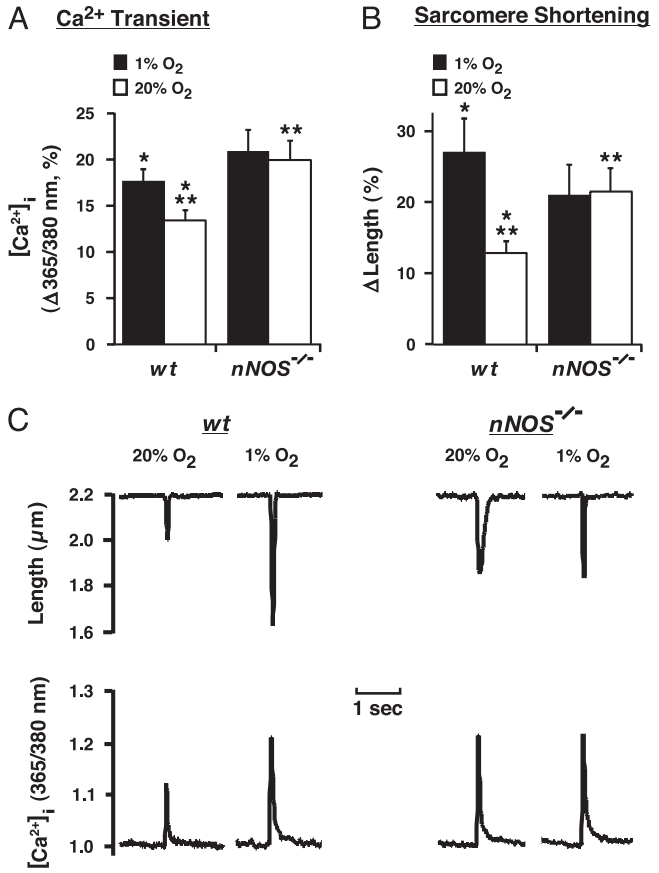

Fig. 4. Ca^{2+} transients (*A*) and sarcomere shortening (*B*) induced by depolarization of myocytes prepared from FDB of WT or *nNOS*$^{-/-}$ mice and stimulated at 1% or 20% O_2. Both measures are significantly greater at 1% vs. 20% O_2 in myocytes from WT mice (*), but there is no effect of pO_2 on either measure in *nNOS*$^{-/-}$ myocytes. Note also that the magnitudes of both Ca^{2+} transients and sarcomere shortening are significantly greater at 20% O_2, but not at 1% O_2, in myocytes from *nNOS*$^{-/-}$ vs. WT mice (**). (*C*) Representative records of cytosolic Ca^{2+} and sarcomere length from an individual WT myocyte and an individual *nNOS*$^{-/-}$ myocyte. Note that the amplitudes of Ca^{2+} transients and of sarcomere shortening are independent of pO_2 in the *nNOS*$^{-/-}$ myocyte.

at higher physiological pO_2. Only the inhibitory influence has been described in previous studies (6) of mammalian striated muscle, which have been conducted exclusively at entirely nonphysiological oxygen tension (95% O_2). Furthermore, because those results (obtained with pharmacological inhibitors) were not consistent with the reported absence of altered muscle function in *nNOS*$^{-/-}$ or nNOS-deficient *mdx* mice (2, 3, 22), the importance of NO in E–C coupling and its potential pathophysiological significance in dystrophic disease have remained in question.

The facilitatory action of NO at normal muscle pO_2 supports the physiological importance of NO-dependent enhancement of calcium release from skeletal muscle SR through *S*-nitrosylation of RyR1 at physiological but not supranormal pO_2, observed *in vitro* (10). In addition, it has recently been shown that endogenous NO enhances RyR-mediated release of Ca^{2+} from SR of cardiac myocytes (23), an action mediated specifically by nNOS (14). The inhibitory effects of NO on contractility at higher pO_2 may reflect the operation of distinct molecular mechanisms, which are revealed most prominently under conditions of oxidative stress. Redox-sensitive muscle proteins that are reported to be modified by NO or S-nitrosoglutathione (GSNO) include the Ca^{2+}-dependent ATPase of the SR (24, 25), which regulates SR-cytosol Ca^{2+} homeostasis, and constituents of the myofilaments (26, 27), which directly subserve contractile function. In addition, activation of guanylate cyclase has been implicated in depression of muscle force by NO/GSNO in previous studies (5, 28) conducted at supraphysiological pO_2.

Regardless of the identity of the full spectrum of proteins acted on by NO/nitrosylation in muscle cells, our experimental results support a model under which the targets, mechanisms of action, and functional effects of endogenous NO will vary continuously with muscle redox status, linked to oxygen tension (and presumably ROS production). The contingent effects of NO would thus couple modulation of contractility to ongoing muscle activity and metabolic demand. Low pO_2 in working muscle would increase contractility and rises in pO_2 in resting muscle would attenuate contractility, which is analogous to the pO_2-dependent regulation of red blood cell-derived NO vasoactivity that couples peripheral blood flow to local metabolic demand (i.e., hypoxic vasodilation and hyperoxic vasoconstriction; refs. 29 and 30). Accordingly, O_2-regulated, NO/S-nitrosothiol-based signals would coordinately regulate both blood flow and contractility in striated muscle beds. This model may apply more generally across cell types and subcellular compartments in which NO-derived bioactivity is exerted, and may thus provide a framework for elucidating the role of NO in redox-based regulation of protein function and cellular physiology (1), which has been largely masked in studies performed to date at supraphysiological pO_2.

Increased force production as a result of oxidative insult (see 95% O_2 in Figs. 2 and 3) or NOS deficiency (Figs. 1, 2, and 3 *F* and *G*) may provide a compensatory mechanism to maintain performance by injured or diseased (dystrophic) muscle. Indeed, it may be the case that chronic deprivation of NO results in oxidative stress. However, this greater force production comes at a price: NO and O_2 no longer exert coordinate control (RyR activity is not regulated by *S*-nitrosylation at supraphysiological pO_2). This broader perspective may provide a novel molecular basis for diverse myopathies that are associated with altered expression, distribution or activity of NOS, and/or impairment of oxygenation or blood flow, previously subsumed under the rubric of oxidative/nitrosative stress, but here viewed as symptomatic of an imbalance in NO/O_2-based signaling that is essential for normal calcium-regulated muscle function. That is, rather than viewing oxidative/nitrosative stress simply in terms of oxidative injury to muscle, our results suggest that impairments in muscle performance may result from physiological alterations in NO/O_2 balance that disrupt nitrosylation/redox-based signaling.

This work was supported by National Institutes of Health Grants HL-59130 (to J.S.S.), HL-04053 (to J.P.E.), and AR-18687 (to G.M.).

1. Stamler, J. S., Lamas, S. & Fang, F. C. (2001) *Cell* **106,** 675–683.
2. Brenman, J. E., Chao, D. S., Xia, H., Aldape, K. & Bredt, D. S. (1995) *Cell* **82,** 743–752.
3. Chao, D. S., Gorospe, G. R., Brenman, J. E., Rafael, J. A., Peters, M. F., Froehner, S. C., Hoffman, E. P., Chamberlain, J. S. & Bredt, D. S. (1996) *J. Exp. Med.* **184,** 609–618.
4. Silvagno, F., Xia, H. & Bredt, D. S. (1996) *J. Biol. Chem.* **271,** 11204–11208.
5. Kobzik, L., Reid, M. B., Bredt, D. S. & Stamler, J. S. (1994) *Nature* **372,** 546–548.
6. Stamler, J. S. & Meissner, G. (2001) *Physiol. Rev.* **81,** 209–237.
7. Thomas, G. D. & Victor, R. G. (1998) *J. Physiol. (London)* **506,** 817–826.
8. Gorczynski, R. J. & Duling, B. R. (1978) *Am. J. Physiol.* **235,** H505–H515.
9. Honig, C. R. & Gayeski, T. E. (1993) *Am. J. Physiol.* **265,** H868–H875.
10. Eu, J. P., Sun, J., Xu, L., Stamler J. S. & Meissner G. (2000) *Cell* **102,** 499–509.
11. Huang, P. L., Dawson, T. M., Bredt, D. S., Snyder, S. H. & Fishman, M. C. (1993) *Cell* **75,** 1273–1286.
12. Close, R. I. (1972) *Physiol. Rev.* **52,** 129–197.

13. Linsenmeier, R. A. & Yancey, C. M. (1987) *J. Appl. Physiol.* **63,** 2554–2557.
14. Barouch, L. A., Harrison, R. W., Skaf, M. W., Rosas, G. O., Cappola, T. P., Kobeissi, Z. A., Hobai, I. A., Lemmon, C. A., Burnett, A. L., O'Rourke, B., *et al.* (2002) *Nature* **416,** 337–339.
15. Sun, J., Xin, C., Eu, J. P., Stamler, J. S. & Meissner, G. (2001) *Proc. Natl. Acad. Sci. USA* **98,** 11158–11162.
16. Reid, M. B., Kobzik, L., Bredt, D. S. & Stamler, J. S. (1998) *Comp. Biochem. Physiol.* **119,** 211–218.
17. Hennig, R. & Lomo, T. (1985) *Nature* **314,** 164–166.
18. Gorassini, M., Eken, T., Bennett, D. J, Kiehn, O. & Hultborn, H. (2000) *J. Neurophysiol.* **83,** 2002–2011.
19. Reid, M. B., Khawli, F. A. & Moody, M. R. (1993) *J. Appl. Physiol.* **75,** 1081–1087.
20. Clanton, T. L., Zuo, L. & Klawitter, P. (1999) *Proc. Soc. Exp. Biol. Med.* **222,** 253–262.
21. Melzer, W., Herrmann-Frank, A. & Luttgau, H. C. (1995) *Biochim. Biophys. Acta* **1241,** 59–116.
22. Chang, W.-J., Iannaccone, S. T., Lau, K. S., Masters, B. S., McCabe, T. J., McMillan, K., Padre, R. C., Spencer, M. J., Tidball, J. G. & Stull, J. T. (1996) *Proc. Natl. Acad. Sci. USA* **93,** 9142–9147.
23. Vila-Petroff, M. G., Kim, S. H., Pepe, S., Dessy, C., Marbán, E., Balligand, J.-L. & Sollot, S. J. (2001) *Nat. Cell Biol.* **3,** 867–873.
24. Xu, K. Y., Huso, D. L., Dawson, T. M., Bredt, D. S. & Becker, L. C. (1999) *Proc. Natl. Acad. Sci. USA* **96,** 657–662.
25. Viner, R. I., Williams, T. D. & Schöneich, C. (2000) *Free Radical Biol. Med.* **29,** 489–496.
26. Perkins, W. J., Han, Y. S. & Sieck, G. C. (1997) *J. Appl. Physiol.* **83,** 1326–1332.
27. Andrade, F. H., Reid, M. B., Allen, D. G. & Westerblåd, H. (1998) *J. Physiol. (London)* **509,** 577–586.
28. Abraham, R. Z., Kobzik, L., Moody, M. R., Reid, M. B. & Stamler, J. S. (1998) *Comp. Biochem. Physiol.* **119,** 177–183.
29. Pawloski, J. P., Hess, D. T. & Stamler, J. S. (2001) *Nature* **409,** 622–626.
30. McMahon, T. J., Moon, R. E., Luschinger, B. P., Carraway, M. S., Stone, A. E., Stolp, B. W., Gow, A. J., Pawloski, J. P., Watke, P., Singel, D. J., *et al.* (2002) *Nat. Med.* **8,** 711–717.